

Numerical Prediction of Lateral Jets for Missile Like Geometries

Ekin Ağsarlıoğlu¹⁾
Ali Akgül¹⁾

Lateral (side) jet control is gaining popularity for maneuvering since it has some advantages over conventional control techniques. At lower dynamic pressure, a lateral-jet controlled missile has more capability for maneuvering than an aerodynamically-controlled missile. Another important advantage is a faster response. In this study, the effects of lateral jets on missile like geometries are investigated numerically by the commercial unstructured Computational Fluid Dynamics (CFD) solver FLUENT. Two generic missile models with side jets, experimental data of which are available in literature, are analyzed. These two models were both tested in the supersonic free-stream and the sonic jet exit conditions in wind tunnels. Model-1 has two different configurations. CFD validations for these configurations are done by comparing the calculated force amplification factor " K " and the interaction moment center " X_{CP} " with the measured values. CFD validations for Model-2 are done by comparing the surface pressure coefficient data at three different roll angles with the measured data. Despite some discrepancies, the experimental data and the CFD results are in good agreement with each other for both generic missile models. As a result, a numerical methodology for solving lateral-jet controlled supersonic missile problems has been developed. This methodology can be used as a part of the lateral-jet controlled missile design.

Key words: missile, missile control, lateral jet, numerical fluid dynamics, numerical simulation.

Introduction

DEFLLECTING the lifting surfaces of a missile, i.e. canards, tails etc., is the conventional way to generate forces and moments for maneuvering purposes. Recently, lateral jet control has been gaining popularity for maneuvering since it has some advantages over conventional control techniques. Firstly, it has a faster response than fin deflections. It is also more effective when flight dynamic pressure is low, i.e. when altitude is high [1]. But the flow field resulting from the interaction of a supersonic free stream and a high pressure jet is very complex. The upstream and downstream regions of the jet exit are affected by the presence of the jet, causing a complex pressure distribution on the surface of the missile.

Flow physics

The flow field resulting from the interaction of the supersonic free stream and the vertically ejecting jet for a 2-D flat plate is shown in Fig.1 [2].

In Fig.1, the jet exit acts like an obstacle to the flow and forms a bow shock. There is also a flow separation upstream of the jet exit. The separation shock and the bow shock form a mixing region. Downstream of the jet, a wake region is formed and a recompression shock exists in order to adjust the free stream back to the horizontal alignment.

For a missile travelling in a supersonic free stream with a side jet, the resulting interaction flow field is shown schematically in Fig.2 [3]. For a missile with a side jet, a jet bow shock and separated region separation shocks also exist. There is another bow shock attached to the nose of

the missile and a mixing region is formed out of the nose and jet bow shocks. A 3-D shock structure is bounded and turned by the mixing layer in the roll direction. The high and low pressure regions form additional forces and moment couples on the missile as a result of the interaction.

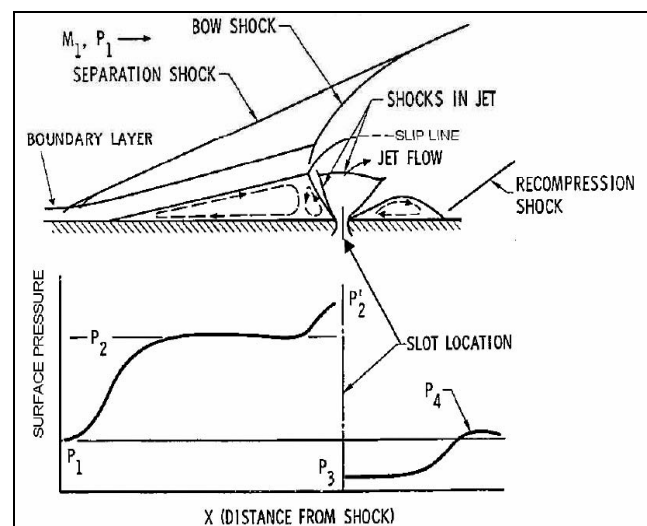


Figure 1. Interaction flow field, 2-D case [2]

As seen in above figures, the interaction flow field is very complex and it has to be analyzed carefully. The flow field contains the shock-shock interaction, the boundary layer-shock interaction zones and the recompression zones which make the CFD analysis more difficult than a conventional missile analysis.

¹⁾ ROKETSAN Missile Industries Inc., P.K.: 30, 06780 Elmadağ-Ankara, TÜRKIYE

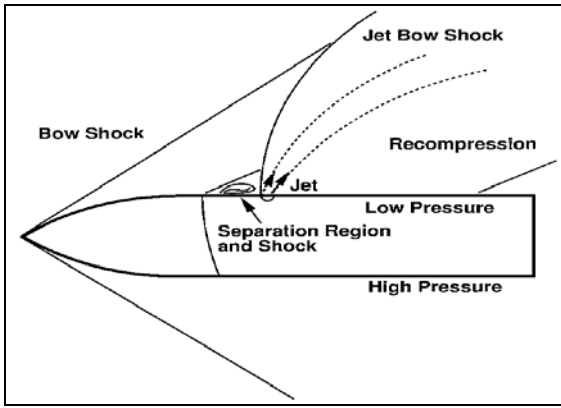


Figure 2. Interaction flow field for a missile [3]

Available experimental data

Two test models from literature are chosen for the validation studies. Their geometric properties and test conditions are given below in detail.

Test Model 1

Test Model-1 [4] (TM-1) is a generic supersonic missile body which has a tangent ogive nose, interchangeable lifting surfaces and a body of a low slenderness ratio. TM-1 is tested for M_∞ from 2 to 8, in presence of angles of attack and for 5 different configurations. But in this study, only the results for Body-Canard (BC) and Body-Tail (BT) configurations at $M_\infty=2$ data are compared with the CFD. TM-1 dimensions for two configurations are shown in Fig.3. The experiments were carried out in the Israeli Aircraft Industries Trisonic Wind Tunnel facility. The ambient and the jet conditions for TM-1 experiments are given in Table 1.

Table 1. TM-1 Test Conditions

Ambient Conditions	
M	2
P [Pa]	24721.2
T [K]	170
Jet Conditions -BC	
M	1
P [Pa]	1821187
T [K]	215
Jet Conditions -BT	
M	1
P [Pa]	1456949
T [K]	235.26

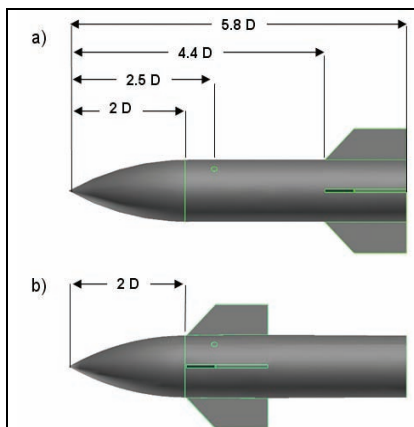


Figure 3. Test Model-1 Dimensions a) Body Tail b) Body Canard

For both configurations, the lifting surfaces are identical. The lifting surfaces have a 45° leading edge sweep angle, $1.4 \times D$ root chord and $0.5 \times D$ semi spans. A sonic circular jet exit is placed $2.5 \times D$ downstream of the nose tip. In Fig. 3, the models are shown in the “+” configuration but in the wind tunnels they were tested in the “x” configuration. The jet stands in the vertical position such that when it is active, it creates negative normal force. As the results of the experiment, the jet force amplification factor K and the interaction moment center X_{CPi} are reported and their definitions are given below.

$$K = \frac{C_{N \text{ jet-on}} - C_{N \text{ jet-off}}}{C_{N \text{ jet}}} \quad (1)$$

$$X_{CPi} = \frac{C_{m \text{ jet-on}} - C_{m \text{ jet-off}}}{(C_{N \text{ jet-on}} - C_{N \text{ jet-off}})} \quad (2)$$

The first equation is a measure of how the interaction forces affect the normal force. If K is greater than unity, the total added normal force to the missile by the jet is greater than the jet alone normal force; thus the jet force is amplified. If it is less than unity, the jet force is de-amplified. X_{CPi} is the measure of the distance where the combination of the interaction and the jet forces act with respect to the moment reference center. It is a characteristic jet interaction moment length scale. For both configurations, the moment reference center is the jet exit location.

Test Model 2

Test Model-2 [5] (TM-2), is a generic supersonic projectile body with a conical nose and a flare after-body. The dimensions are given in Fig.4. The experiments were carried out in the DLR wind tunnel in Cologne, Germany. The ambient and the jet conditions for the wind tunnel experiments are given in Table 2.

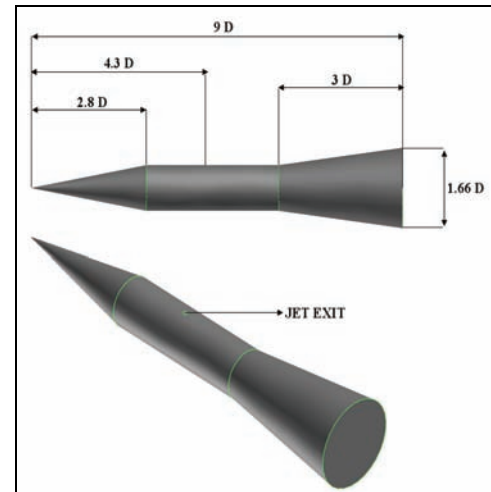


Figure 4. TM-2 Dimensions

Table 2. TM-2 Test Conditions

Ambient Conditions	
M	2.8
T [K]	108.96
P [Pa]	20793.2
Jet Conditions	
M	1
$P_{\text{jet}}/P_{\text{ambient}}$	100

In the experiments, M_∞ is set to 2.8 and a 0.1 caliber circular sonic jet exit is placed 4.3 calibers behind the nose tip. The jet is sonic and the pressure coefficient data for roll angles (φ) 180°, 150° and 120° are reported. The sign convention used in this study is shown in Fig.5.

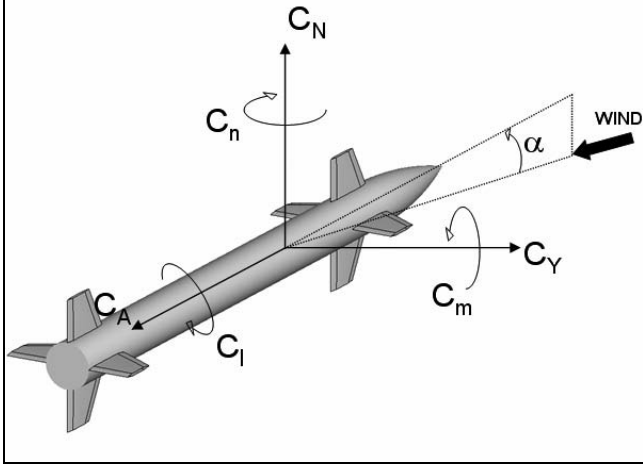


Figure 5. Sign Convention

Grid generation

The computational grid is generated in three steps. GAMBIT is used for the surface grid generation. Then TGrid is used for creating the boundary layer mesh. Finally, GAMBIT is used again to generate the volume mesh. Triangular elements are used for the surface grid, wedge elements are used for the boundary layer grid and tetrahedral elements are used for the volume grid. As a result, the mesh file is exported to FLUENT for CFD simulations.

According to published works in literature [6,10,11], the mesh has to be very fine around the jet exit for capturing the shocks and high magnitude gradients. The surface and the volume grid around the jet have been made finer by using sizing functions. The boundary layer grid was so prepared that the cells closest to the wall boundary condition zones had the y^+ value around 1 [7]. In Figs. 6-8; the surface, the boundary layer and the volume grid for TM-1 are shown.

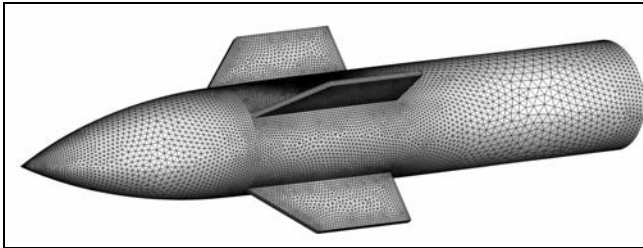


Figure 6. TM-1-BC, Surface Grid

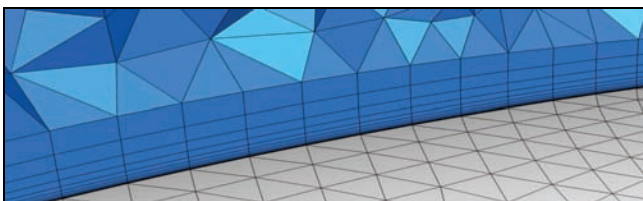


Figure 7. TM-1-BC, Boundary Layer Grid

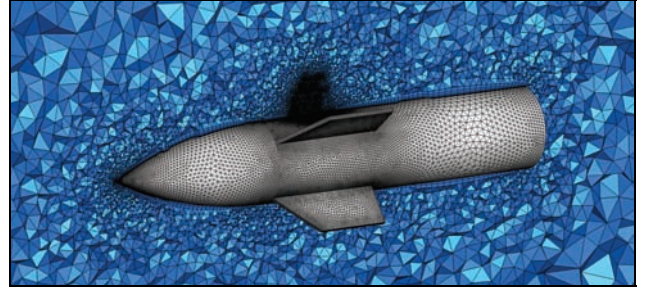


Figure 8. TM-1-BC, Volume Grid

The computational grid contains around 3 million cells for two configurations. For TM-2, the volume grid contains around 6 million cells. Convergence was not achieved for TM-1 with a smaller grid size. The CFD simulations are continued until changes in the axial force, the normal force and the pitching moment coefficients for successive iterations are less than %1.

Boundary conditions and solution strategy

In numerical simulations, a steady, density-based solver option is used with $k-\epsilon$ realizable and $k-\omega$ turbulence models [8]. Conservation equations are solved by the finite volume technique.

$$\frac{\partial}{\partial t} \int_V W dV + \oint [F - G] \cdot dA = \int_V H dV \quad (3)$$

$$W = \begin{Bmatrix} \rho \\ \rho u \\ \rho v \\ \rho w \\ \rho E \end{Bmatrix}, F = \begin{Bmatrix} \rho v \\ \rho v u + p i \\ \rho v v + p j \\ \rho v w + p k \\ \rho v E + p v \end{Bmatrix}, G = \begin{Bmatrix} 0 \\ \tau_{xi} \\ \tau_{yi} \\ \tau_{zi} \\ \tau_{ij} v_j + q \end{Bmatrix} \quad (4)$$

The inviscid flux vector F is evaluated by a standard upwind flux-difference splitting. In the density-based solver, each equation in the coupled set of governing equations is linearized implicitly with respect to all dependent variables in the set, resulting in a block system of equations. A block Gauss-Seidel, point implicit linear equation solver is used with an algebraic multigrid method to solve the resultant block system of equations. Second-order discretization was used for all flow variables.

For CFD calculations, a large cylindrical domain with 50 model lengths in the axial direction and 18 model lengths in a diameter is created for the flow field. The “Pressure Far Field” boundary condition is defined for faces of the cylindrical domain. The “Wall” boundary condition with no slip is selected for model surfaces and the “Mass Flow Inlet” is selected for the jet-exit. The analysis takes about 10 hours for a single case for TM-1 and 20 hours for TM-2. Every case was run on a node of a cluster, which has 8 processors 24 GB of RAM.

Results and comparison

In the following sections, the CFD predictions and comparison with the experimental results are given.

Test Model 1

A turbulence model study is conducted by using the Body Canard configuration in the entire angle of attack

range. Realizable $k-\varepsilon$ and $k-\omega$ models are selected for this study. The results of the turbulence model study are given in Figs. 9-10.

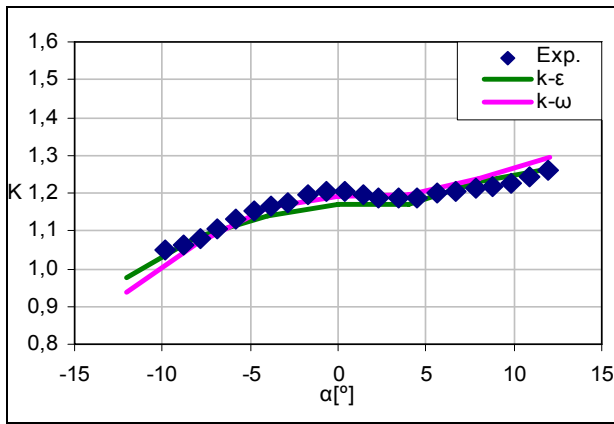


Figure 9. TM-1-BC, Turbulence Model Study - Comparison of K values

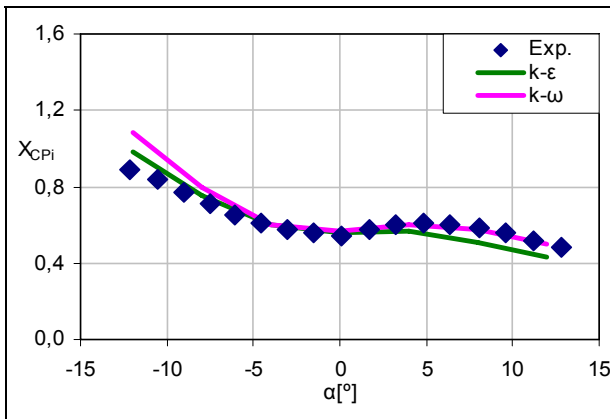


Figure 10. TM-1-BC, Turbulence Model Study - Comparison of $X_{C_{Pi}}$ values

If the above Figures are examined, both turbulence models agree well with the experimental data. The maximum error for the $k-\varepsilon$ model is less than %13 for $X_{C_{Pi}}$, whereas less than %21 for $X_{C_{Pi}}$ in the $k-\omega$ model. It takes about %50 more iterations for $k-\omega$ simulations to reach convergence than for $k-\varepsilon$ simulations. Considering the maximum errors and the ease of convergence, the $k-\varepsilon$ model is selected to be used for the rest of the study.

The results for the Body Tail configuration are shown in Figs. 11 -12.

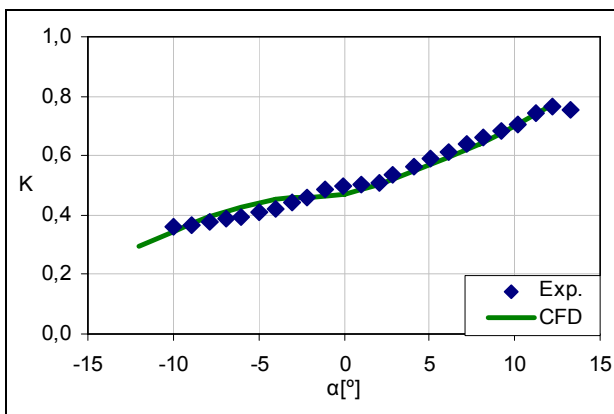


Figure 11. TM-1-BT, Comparison of K values

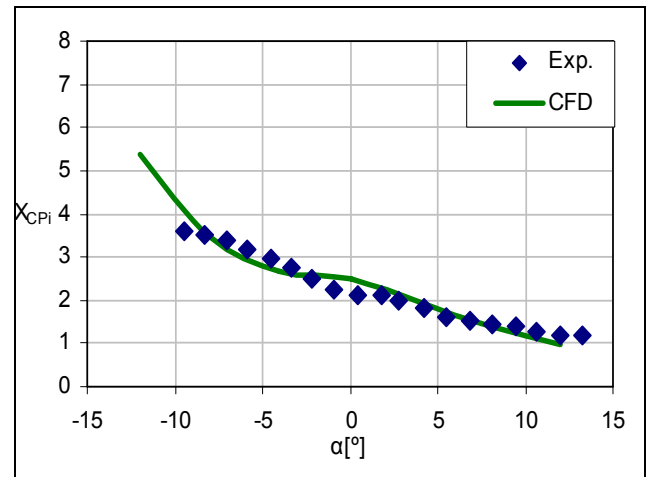


Figure 12. TM-1-BT, Comparison of $X_{C_{Pi}}$ values

In the Body Tail configuration, the maximum error is less than %14 for K values around zero angle of attack. There is agreement between the CFD and the experimental results also for this configuration.

In the K curves, for BC configuration K is greater than 1 in the entire angle of attack range whereas in the BT configuration, it is less than 1. It means that for the former configuration the jet-alone normal force is amplified whereas in the latter configuration it is de-amplified. In Figs. 13 and 14, the static pressure distribution around the model and the pitch plane is shown. If these figures are examined, the low pressure region caused by the jet is larger in the BT configuration than in the BC configuration. This lower pressure indicates that total normal force acting on the model decreases. Also in the BC configuration, pressure is increased on the upper surface of the canards; more negative normal force is thus generated. Due to these two factors, negative normal force is further increased in the BC configuration. It is also evident that for negative angles of attack, force amplification decreases for both configurations. Noted by several authors [9], in negative angles of attack, the jet wake is directed to lifting surfaces and decreases the pressure on the upper surfaces of canards or tails. Thus normal force contribution of these parts decreases and force amplification decreases.

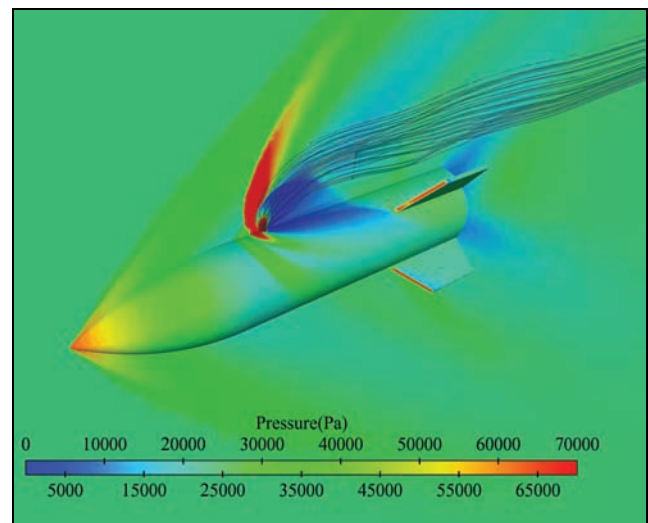


Figure 13. TM-1-BT, Surface Pressure Contours in Plane and Jet Exit Streamlines

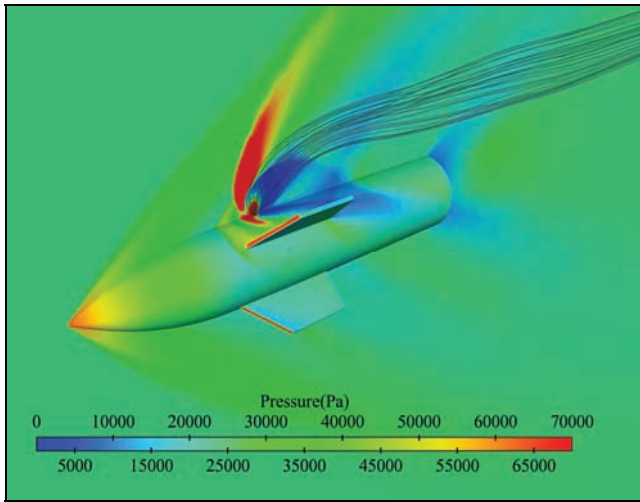


Figure 14. TM-1-BC, Surface Pressure Contours in Plane and Jet Exit Streamlines

Test Model 2

For TM-2, C_p values are compared for $\varphi = 180^\circ, 150^\circ$ and 120° . The comparative results are shown in the following Figures. The surface pressure is non-dimensionalized by the free stream dynamic pressure and the cross section area.

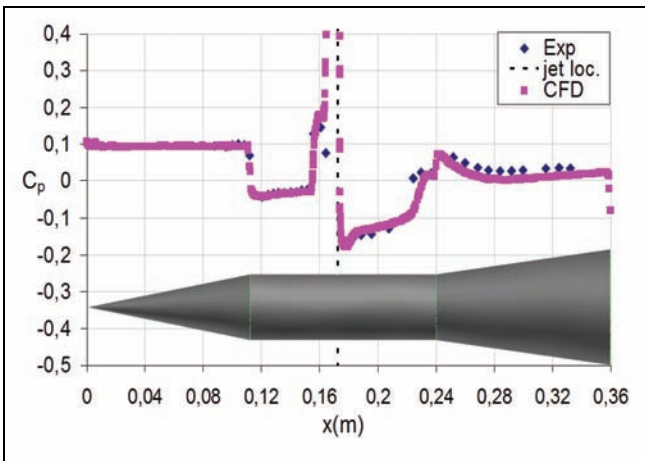


Figure 15. TM-2, C_p Comparison, $\varphi = 180^\circ$

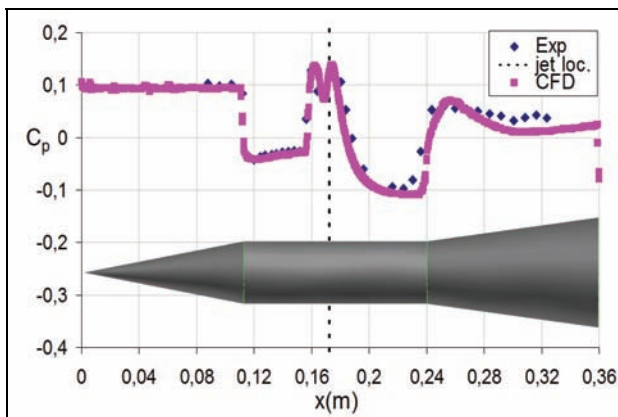


Figure 16. TM-2, C_p Comparison, $\varphi = 150^\circ$

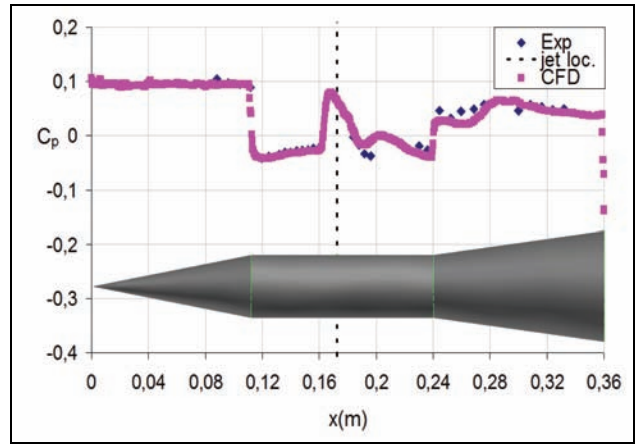


Figure 17. TM-2, C_p Comparison, $\varphi = 120^\circ$

If the surface pressure coefficients from the CFD and the experiments for different roll angles are examined, the CFD results are in good agreement with the experimental data. Some discrepancies exist in the flare part downstream and the separation part just upstream of the jet exit. The maximum error is about %10 for the surface static pressure value for 120° roll angle at about $x = 0.2$ m. The static pressure and the Mach number contours around the model are shown in the following Figures.

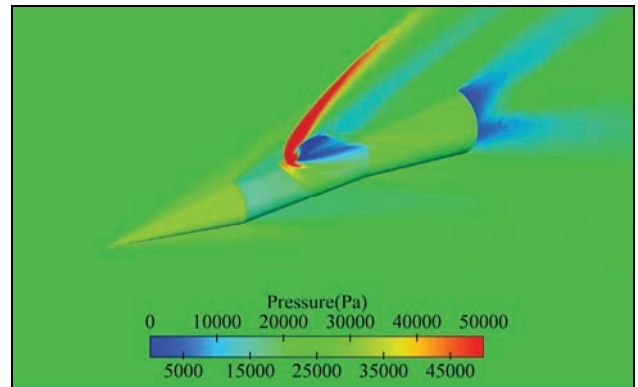


Figure 18. TM-2, Static Pressure Distribution

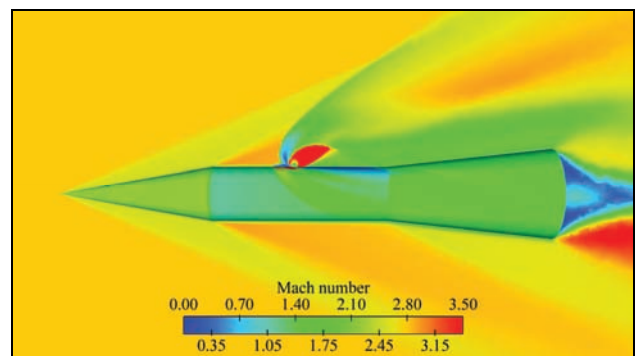


Figure 19. TM-2, Mach Number Distribution Around Model and Static Pressure Distribution on Model

As stated before, the flow field is very complicated in the vicinity of the jet. In Fig.20, there is a close up view of the jet exit. The Figure contains the jet exit streamlines and the Mach number contours in the pitch plane.

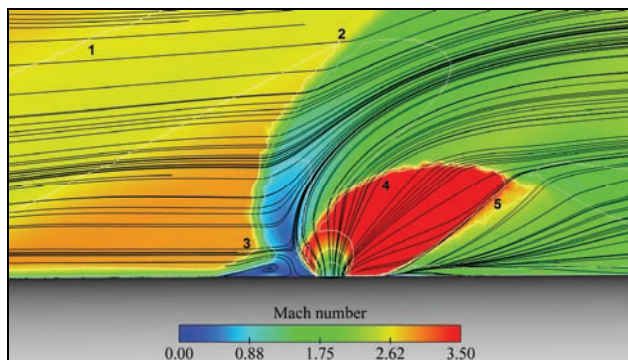


Figure 20. TM-2, Flow Field around the Jet Exit,

In Fig.20, 1 is the nose bow shock. 2 is the jet bow shock and 3 is the upstream separation zone. 4 is the jet expansion region caused by high speed jet exiting to the free stream. Finally, 5 is the recompression shock to orient the flow parallel to the model. If Fig.20 is compared with Fig.2, it may be seen that the prominent flow features of the jet interaction problem are captured by the CFD simulations.

Conclusions and future work

In this study, numerical investigation of lateral jets was done with the commercial CFD solver FLUENT. Validation studies were carried out for two generic side jet controlled missile like models. For TM-1, the calculated force amplification factor “K” and the interaction moment center “ X_{Cp_i} ” were compared with the experimental values. For TM-2, the surface pressure coefficients at different roll angles were compared with the experimental values. The calculated values for both models are in good agreement with the experimental data. The maximum error for TM-1 is less than %14 for K value in the BT configuration and less than %13 for X_{Cp_i} value for the BC configuration. The maximum error for TM-2 is less than %10 for the surface static pressure. These error margins are very small for these complex flows and can be acceptable for the design of lateral jets. With the techniques and software used in this study, it might be concluded that numerical methodology has been validated for the solution of the side-jet and supersonic free stream interaction problem.

As a future work, a series of CFD simulations will be carried out to form a database for a generic supersonic missile with a side jet. Input parameters to the database will be the angle of attack, the jet location and the jet mass flow

rate. As a result, the force and moment values of missile parts in the pitch plane will be obtained. The influences of these parameters on the forces and moments of missile parts will be investigated. A side-jet controlled missile aerodynamic design tool will be developed using the database and the influence factors between jet parameters and forces and moments of missile parts. This tool will be used in the preliminary design phase of a side-jet controlled missile.

Acknowledgements

The authors thank ROKETSAN for supporting this research.

REFERENCES

- [1] HITZEL, S.M.: *Navier-Stokes Simulations around a High Velocity Missile with Cross Flow Jet*, RTO AVT Symposium on Missile Aerodynamics, Sorrento, Italy, 1998.
- [2] CASSEL, L.A.: *Applying Jet Interaction Technology*, AIAA Journal of Spacecraft and Rockets, July – August 2003, Vol.40, No.4.
- [3] GRAHAM, M.J., WEINACHT, P.: *Numerical Investigation of Supersonic Jet Interaction for Axisymmetric Bodies*, AIAA Journal of Spacecraft and Rockets, September-October 2000, Vol.37, No.5.
- [4] BRANDEIS, J., GILL, J.: *Experimental Investigation of Super and Hypersonic Jet Interaction on Missile Configurations*, AIAA Journal of Spacecraft and Rockets, May-June 1998, Vol.35, No.3.
- [5] GNEMMI, P., ADELLI, R.: *Computational Comparisons of the Interaction of a Lateral Jet on a Supersonic Generic Missile*, AIAA Atmospheric Flight Mechanics Conference and Exhibit, Honolulu, Hawaii, 2008.
- [6] SRIVASTAVA, B.: *Lateral Jet Control of a Supersonic Missile: Computational and Experimental Comparisons*, AIAA Journal of Spacecraft and Rockets, March-April 1998, Vol.35, No.2.
- [7] GERASIMOV, A.: *Modeling Turbulent Flows with FLUENT*, ANSYS, 2006.
- [8] ANSYS Fluent User's Guide, April 2009.
- [9] GRAHAM, M.J., WEINACHT, P., BRANDEIS, J., ANGELINI, R.: *A Numerical Investigation of Supersonic Jet Interaction for Finned Bodies*, ARL Report, 2000.
- [10] GÜLAY, E., AKGÜL, A., ISAKOVIĆ, J., MANDIĆ, S.: *CFD and Experimental Investigation of Wrap-Around-Fins Missile Rolling Moment*, Scientific Technical Review, ISSN 1820-0206, 2011, Vol.61., No.3-4, pp.8-15.
- [11] AKGÜL, A. at all.: *Numerical Investigation of NASA Tandem Control Missile and Experimental Comparison*, Scientific Technical Review, ISSN 1820-0206, 2012, Vol.62., No.1, pp.3-9.

Received: 09.03.2012.

Numerička simulacija bočnih mlazeva na projektilima

Upravljanje bočnim mlazovima za manevrisanje, dobija na sve većoj popularnosti pošto ima neke prednosti u odnosu na konvencionalne metode upravljanja. Pri nižim dinamičkim pritiscima projektili koji su upravljani bočnim mlazovima, imaju veću sposobnost manevrisanja u odnosu na aerodinamički upravljane projekte. Druga važna prednost je brži odgovor. U ovoj studiji, efekat bočnih mlazeva na projektilima se istražuje numerički sa nestrukturisanim solverom FLUENT za numeričku dinamiku fluida. Dva generička modela sa bočnim mlazovima za koje postoje eksperimentalni podaci u literaturi, su analizirana. Ova dva modela su bila testirana u aerotunelima za nadzvučne brzine strujanja i sonične uslove na izlazu mlaza. Model 1 ima dve različite konfiguracije. CFD potvrde za ove konfiguracije su učinjene poredeći izračunati faktor pojačanja sile K, i centar momenta interakcije X_{cp} , sa merenim vrednostima. CFD potvrde za Model 2 su učinjene poredeći podatke za koeficijent pritiska na površini za tri različita ugla valjanja, sa merenim podacima. Uprkos izvesnim neslaganjima, eksperimentalni podaci i CFD rezultati se dobro slažu za oba generička modela projektila. Kao rezultat, razvijena je numerička metodologija rešavanja problema upravljanja supersoničnih projektila pomoću bočnog mlaza. Ova metodologija može se koristiti kao deo konstruisanja projektila upravljanih bočnim mlazom.

Ključne reči: projektil, upravljanje projektilom, bočni mlaz, numerička dinamika fluida, numerička simulacija.

Численное моделирование боковой струи в снарядах

Управление боковыми потоками в сторону манёвренности, завоевывает все большую популярность, так как имеет ряд преимуществ по сравнению с традиционными методами управления. При низком динамическом давлении снаряды, управляемые боковыми струями, имеют большую манёвренность, чем аэродинамически контролируемые ракеты. Другим важным преимуществом является более быстрый отклик. В этом исследовании, эффект боковых струй в ракетах исследуется численно с неструктурированным решателем FLUENT для численной гидродинамики. Здесь анализируются две общих генерических модели с боковыми потоками, для которых имеются экспериментальные данные в литературе. Эти две модели были испытаны в аэродинамической трубе для сверхзвуковых скоростей потока и для звуковых условий на выходе потока. Модель 1 имеет две различные конфигурации. CFD подтверждения для этих конфигураций рассчитываются путём сравнения коэффициента усиления силы K , крутящего момента и центра взаимодействия ХСР, с измеренными значениями. CFD подтверждения для Модели 2 рассчитываются путём сравнения данных для коэффициента поверхностного давления для трёх различных углов крена, с измеренными данными. Несмотря на некоторые разногласия, экспериментальные данные и результаты CFD соответствуют общим для обеих моделей ракет. В результате разработана численная методология решения проблем управления сверхзвуковых ракет при помощи боковых струй. Эта методология может быть использована как часть построения ракет контролируемых боковой струей.

Ключевые слова: снаряд, управление снарядом, боковой поток (струя), численная гидродинамика, численное моделирование.

Simulation numérique des jets latéraux chez les missiles

Le contrôle des jets latéraux pour les manœuvres devient de plus en plus populaire car il offre certains avantages par rapport aux autres méthodes conventionnelles de contrôle. Au cours des pressions dynamiques plus basses les missiles contrôlés par les jets latéraux ont plus grande capacité de manœuvre par rapport aux missiles contrôlés de façon aérodynamique. L'autre avantage est une réponse plus rapide. Dans cette étude l'effet des jets latéraux chez les missiles est étudié numériquement à l'aide d'un solveur FLUENT non structuré pour la dynamique numérique des fluides. Deux modèles génériques aux jets latéraux pour lesquels existent les données expérimentales dans la littérature ont été analysés. Ces deux modèles ont été testés dans les souffleries aérodynamiques pour les vitesses supersoniques des courants et pour les conditions soniques à la sortie du jet. Le modèle 1 a deux configurations différentes. Les confirmations CFD pour ces deux configurations ont été effectuées par la comparaison du facteur calculé K de l'amplification de force et du centre de moment de l'interaction Хср avec les valeurs mesurées. Les validations CFD pour le modèle 2 ont été effectuées en comparant les données pour le coefficient de pression sur la surface pour trois différents angles de roulement avec les données mesurées. Malgré certaines discordances, les données expérimentales et les résultats CFD sont en bon accord pour les deux modèles génériques des missiles. Comme le résultat on a développé la méthodologie numérique pour la résolution des problèmes du contrôle des missiles supersoniques par le jet latéral. On peut utiliser cette méthodologie comme une part de la conception des missiles contrôlés par le jet latéral.

Mots clés: missile, contrôle de missile, jet latéral, dynamique numérique des fluides, simulation numérique.